Phase Morphology and Compatibilization Mechanism in Ternary Polymer Blend Systems of Polyethylene Terephthalate, Polyolefin Rubber, and Ionomer

Hiroshi Ohishi

Advanced Technology Research Laboratories, Nippon Steel Corporation, 20–1 Shintomi, Futtsu, Chiba, 293-8511, Japan

Received 16 July 2003; accepted 18 February 2004
DOI 10.1002/app.20636
Published online in Wiley InterScience (www.interscience.wiley.com).

ABSTRACT: The phase morphology and the mechanism of the compatibilization in ternary blends of PET/EBM (ethylene buten rubber)/ionomer (partially neutralized ethylene and methyl methacrylic acid copolymer, EMAA) are examined. Applying the repulsion idea in random copolymer, the ionomer was selected as an encapsulating agent to compatibilize PET/EBM blend. As anticipated, the ionomer can encapsulate EBM in PET matrix and effectively compatibilize PET and EBM. The results of droplet sandwich experiments verified that the actual driving force for the encapsulation is wettability. In addition, this wettablility was found to be realized by the contribution of the polar and nonpolar units in the ionomer: The polar units decrease the interfacial tension between PET and the ionomer, and the nonpolar units decrease that between EBM and the ionomer. The metal ions in the ionomer have little influence on the wettability, and consequently EMAA can encapsulate EBM even when unneutralized. The efficiency of the compatibilization, on the other hand, is not determined by the wettability only, and the metal ions play an important role. EMAA can effectively compatibilize EBM and PET only when neutralized. This compatibilization effectiveness of the ionomer is supposedly due to the strong interaction between PET and the metal ions. J Appl Polym Sci 93: 1567–1576, 2004

Key words: polyesters; polyolefin; blends; compatibilization; encapsulation

INTRODUCTION

Polymer blending is a simple and efficient method for designing and controlling performance of polymeric materials using easily available polymers. The procedure makes it possible to develop a new polymeric material of synergetic performance of each polymer, to reduce the cost of engineering plastics by diluting them with lower cost polymers, or to enhance recycling of used plastics. These advantages of polymer blending on performance, economy, and ecology have accelerated research and development activities in the field of polymer blends and alloys in terms of both academic and industrial interests.[1–5]

We have carried out research and development of polymer blends mainly based on polyethylene terephthalate (PET) as a part of an effort in developing a new high performance polymer for metal coating. PET is an important engineering polymer used in a wide variety of applications, such as packaging, electronics, and coating for metal because of its excellent balance of properties, including transparency, barrier properties, and thermal and chemical stability. However, PET has some deficient characteristics that deter its use in some areas. When applied for metal surface coating, the PET film is often laminated on the metal plate surface directly at a higher temperature than the melting point.[6–8] Afterward, the metal plate undergoes severe molding processes such as draw and ironing to form the desired shape.[6–8] If small delaminating or cluck arises on the laminated film during these processes, the metal plate will easily crust in practical use. When an orientated PET film is utilized, the retained orientation stress often causes the delaminating, although it satisfies the toughness required for these severe processes. While without any orientation, fragility in the amorphous phases of PET film often causes defects during the molding process. Hence, coexistence of toughness and good adhesion to the metal has been extensively studied in applying PET films to metal coating.

In this research, we have attempted to apply a ternary blend system of PET, ethylene–buten—rubber (EBM), and ionomer (partially neutralized ethylene and methyl methacrylic acid copolymer, EMAA) to the metal coating. By blending PET with EBM, the PET film should be applicable without any orientation, because the dispersed EBM phase should reinforce the fragility in the amorphous phase. However, because PET and EBM are completely immiscible, an adequate compatibilization is necessary.[9–13] Furthermore, be-

Correspondence to H. Ohishi (hohishi@re.nsc.co.jp).

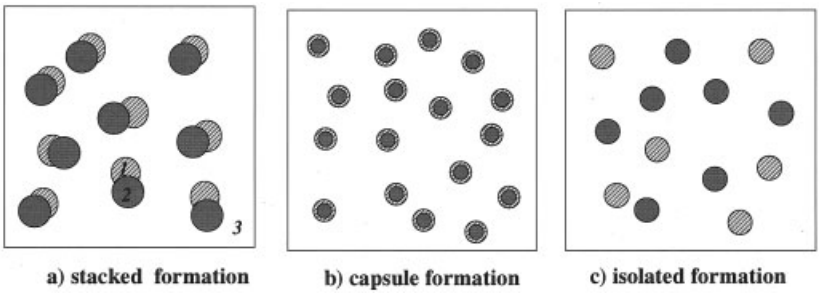

Figure 1 Possible morphology formation in ternary polymer blends. (a) Stacked formation; (b) capsule formation; (c) isolated formation.

cause EBM is nonpolar, the dispersed EBM phase should be avoided to contact directly with the metal from an adhesion viewpoint. To solve these problems, an ionomer was selected as a compatibilizer. According to the molecular design concept mentioned later, the ionomer has a potential to encapsulate EBM in PET matrix. By encapsulating the EBM phase with the ionomer, the interface between the EBM and PET should be stabilized, leading to finer dispersed domains. In addition, the polar units in the encapsulating ionomer should compensate the adhesion of the film, because the ionomer should directly contact with the metal surface in place of the dispersed EBM phase.

In this article, we introduce the molecular design concept for an encapsulating agent and then examine the phase morphology of a ternary blend system of PET, EBM, and the ionomer. Furthermore, to verify the molecular design concept, the mechanism for encapsulation and compatibilization in this blend is experimentally examined in detail.

MOLECULAR DESIGN CONCEPT FOR THE ENCAPSULATING AGENT

An encapsulating agent for the PET and EBM blend system was designed by combing the following three concepts:

1. driving force for encapsulation is wettability.[14–18]
2. interfacial tension between two polymers can be controlled by the (Flory–Huggins) interaction parameter, χ.[19,20]
3. χ parameter can be controlled by an adequate random copolymerization.[21–24]

Driving force for encapsulation

In a ternary polymer blend system where two minor phases are dispersed in a continuous matrix, there are three possible kinds of formation.[15–18] They are shown schematically in Figure 1:

1. "stack formation" of ***1*** and ***2*** stuck together,
2. "capsule formation" of ***2*** encapsulated by ***1***, and
3. "isolation formation" of ***1*** and ***2*** dispersed separately.

Most of ternary immiscible polymer systems form the stack formation.[15–18] Only when polymer ***1*** is wettable between polymer ***2*** and polymer ***3***, the encapsulation of Figure 1(b) occurs. The wettability can be evaluated by the spreading coefficient, $\lambda_{1/2 \text{ in } 3}$, in eq. (1) at a first approximation. Equation (1) was obtained by rewriting the Harkin's equation by Hobbs:[14]

$$\lambda_{1/2 \text{ in } 3} = \gamma_{2/3} - \gamma_{1/2} - \gamma_{1/3} \quad (1)$$

where $\gamma_{2/3}$, $\gamma_{1/2}$, and $\gamma_{1/3}$ are the interfacial tensions between polymers ***1***, ***2***, and ***3*** indicated in Figure 1. When $\lambda_{1/2 \text{ in } 3}$ is positive, ***1*** is wettable between polymer ***2*** and polymer ***3***, and consequently the capsule formation of Figure 1(b) could be developed.[14]

Control of interfacial tensions

The interfacial tensions, $\gamma_{i/j}$, in eq. (1) are determined by the force balance between the self-aggregation in each polymer and the affinity to the other polymer, leading to the following expression:[19,20]

$$\gamma_{i/j} = kT/a^2(\chi_{i/j}/6)^{1/2}[1 - \pi^2/(12\chi_{i/j})(1/N_i + 1/N_j)] \quad (2)$$

$$\sim kT/a^2(\chi_{i/j}/6)^{1/2} \quad (3)$$

where k is Boltzmann coefficient; $\chi_{i/j}$ is the interaction parameter between polymers ***i*** and ***j***; a is the statistical segment (monomer) length; N_i is polymerization degree of polymer ***i***. Because N_i in most polymers is large, the second and third terms in eq. (2) could be neglected compared to the first term. As a result, $\gamma_{i/j}$ is evaluated to be proportional to the square root of $\chi_{i/j}$ as in eq. (3). By substituting eq. (3) into eq. (1), $\lambda_{1/2 \text{ in } 3}$ is approximated by eq. (4):

$$\sqrt{6}a^2/kT\lambda_{1/2\text{ in }3} \sim \chi_{2/3}{}^{1/2} - \chi_{1/2}{}^{1/2} - \chi_{1/3}{}^{1/2} = \chi_{\text{EBM/PET}}{}^{1/2} - \chi_{1/\text{PET}}{}^{1/2} - \chi_{1/\text{EBM}}{}^{1/2} \quad (4)$$

where polymers ***2*** and ***3*** are EBM and PET, respectively. Because PET and EBM are polar and nonpolar, respectively, $\chi_{\text{PET/EBM}}$ should be large. Therefore, if polymer ***1*** is designed to have small χ to both PET and EBM, $\lambda_{1/\text{EBM in PET}}$ should become positive.

Control of χ by random copolymerization

The χ of polymer ***1*** to both PET and EBM can be controlled by an adequate random copolymerization.[21–25] This concept is interpreted by recent idea of "repulsion" in random copolymers in relation to "miscibility window."[21–25] According to the repulsion idea, χ between polymer ***i*** and the random copolymer consisting of monomeric units, ***a/b***, is formulated by eq. (5):[22–24]

$$\chi_{ab/i} = \phi_a\chi_{a/i} + (1 - \phi_b)\chi_{b/i} + \phi_a(1 - \phi_a)\chi_{a/b} \quad (5)$$

where φ_a is volume fraction of unit ***a*** in the random copolymer. Because the last term is subtracted in eq. (5), it contributes favorably to a decreased $\chi_{ab/i}$ when$\chi_{a/b}$ is large. The larger $\chi_{a/b}$ is, the smaller $\chi_{ab/i}$. This signifies the larger the internal repulsion in random copolymer is, the more favorably a quasiattractive force will work between the random copolymer and polymer ***i***. By attracting polymer ***i*** into the random copolymer phase, the repulsive field within the random copolymer will be stabilized.

Applying this concept to the molecular design and selecting a random copolymer consisting of nonpolar and polar units as polymer ***1***, both $\chi_{1/\text{PET}}$ and $\chi_{1/\text{EBM}}$ can be controlled small from the following reasons. Because the units ***a*** and ***b*** are polar and nonpolar, respectively,$\chi_{a/b}$ should be large. In addition, because PET is a polar polymer, $\chi_{a/\text{PET}}$ should be small. Consequently, $\chi_{ab/\text{PET}}$ could become small because of large $\chi_{a/b}$ and small$\chi_{a/\text{PET}}$ in eq. (5). While, because EBM is nonpolar, $\chi_{b/\text{EBM}}$ should be also small. As a result, $\chi_{a/\text{EBM}}$ also becomes small because of large$\chi_{a/b}$ and small$\chi_{b/\text{EBM}}$.

On the basis of the combination of these three concepts, the ionomer was selected as the encapsulating agent for EBM in PET matrix. The ionomer is a random copolymer whose nonpolar and polar units are ethylene and partially neutralized methacrylic acid, respectively.

EXPERIMENTAL

Materials

All of the materials were supplied from commercial sources. Copolymer PET in pellet form (I. V. = 1.09, isophthalic acid mol % = 8) was obtained from Unitika Co. Japan (SA-1346P). EBM was supplied from JSR Japan (EBM 2041P), whose buten content was about 20 wt %. EMAA (a special grade) and the ionomers were obtained from Dupont-Mitsui Polychem. Co. Ltd. Japan. They consist of ethylene and methacrylic acid and supposedly have almost the same composition. The composition is roughly 90 vol % of ethylene and 10 vol % of methacrylic acid. The ionomers were partially neutralized with zinc (I-Zn: Himilan 1706), sodium (I-Na: Himilan 1707), and magnesium (I-Mg: a special grade), respectively, with the neutralization ratio approximately 60%. However the exact MAA composition and its neutralization ratio in these polymers are unknown. Very-low-density polyethylene (VLDPE: SP0540) was obtained from Mitsui Chem. Co., Ltd., Japan.

Melt mixing and morphology observation

All of the polymer blends were intensively melt mixed by a corotating twin-screw extruder (Japan Steel Works Corp., Japan, TEX30SS, 30-mm diameter, L/D = 50, 120 rpm) at a feed rate of 15 kg/h under 270°C of barrel temperature, and then pelletized. Before each processing experiment, all the polymeric materials were dried for at least 24 h at 80°C in a vacuum oven to ensure complete removal of sorbed water.

The blend morphologies were examined by a scanning electron microscope (SEM) and a transmission electron microscope (TEM). For SEM observation, the pelletized specimens were fractured in liquid nitrogen, followed by *meta*-xylene etching at 130°C for 30 min to extract the polyolefin-rich phases. The etched specimens were washed several times by distilled water, followed by drying. The etched surface was coated with gold (30 nm in thickness). Only when the phase morphologies in the EBM/ionomer and the EBM/VLDPE blend systems were analyzed, the fractured face was observed without any etching process. In the SEM micrographs, the darker portions were assigned to the polyolefin-rich phases that were eliminated by the etch ant, while the brighter portions were assigned to the PET-rich phases.

For TEM observation microtomed films were obtained from the pelletized specimens. They were stained with osmium tetra-oxide vapor for 1 day at room temperature. The TEM observation was carried out using a Hitachi TEM, H-7100FA at an accelerating voltage of 100 kV. In the TEM micrographs, each phase was distinguished by contrast in the strained color, because the stained color should fade in the order of VLDPE, the inomomer, EBM, and PET-rich phase, corresponding to the decrease in ethylene residue content. The darkest, gray, and brighter potions were attributed to VLDPE or the ionomer, EBM, and PET-rich phases, respectively.

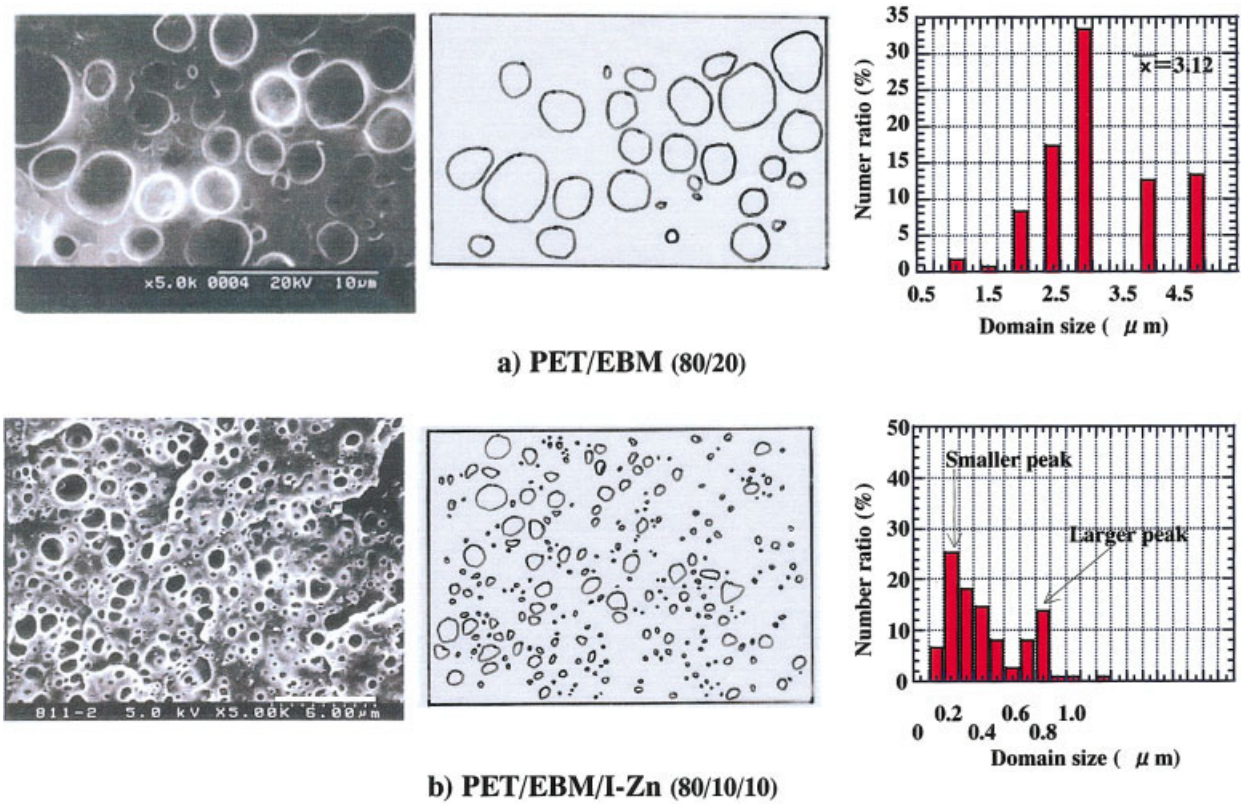

Figure 2 SEM micrographs, binary images, and size distribution of the dispersed domains in (a) PET/EBM (80/20) and (b) PET/EBM/I-Zn (80/10/10) blends. Numbers in parentheses indicate blend composition by weight.

Droplet sandwich experiment[15,18]

Small specimens (about 0.5 × 0.5 mm) were sandwiched with the flat sheets of the other two polymers. The sheets were then annealed at 270°C for 30 min on the hot stage, Limkam TH-600RH, under nitrogen atmosphere. Afterward, the sheets were quickly cooled with liquid nitrogen, and then the cross sections were observed under the microscope to evaluate the shape and location of the sandwiched pieces between the two polymers.

RESULTS AND DISCUSSION

Phase morphology in PET/EBM/I-Zn blends

Figure 2 shows the SEM micrographs, binary images, and size distributions of PET/EBM (80/20) and PET/EBM/I-Zn (80/10/10) blends. In the PET/EBM blend, EBM-rich phases dispersed in PET matrix larger than 3 μm. In addition, the size seems relatively monodispersed. While, in the ternary blend of the PET/EBM/I-Zn, the size of the EBM or the I-Zn rich phases is reduced below 1 μm. This signifies that I-Zn effectively compatibilizes PET and EBM blend systems. Furthermore, there seem to be two size distributions of the dispersed phases. One is around 0.2 μm, and the other around 0.8 μm. However, further analysis of phase molophology is impossible, because in the SEM micrographs both the EBM and the I-Zn rich phases were eliminated by *m*-xylene.

To distinguish each of the three phases and to analyze the morphology formation more clearly, Figure 3 shows the TEM micrographs of the PET/EBM/I-Zn blend. In the TEM micrographs, there are two kinds of dispersed domains. One is a gray domain encapsulated with darker portion. From the contrast of the stained color, these domains can be attributed to the EBM-rich phase encapsulated with the I-Zn-rich phase. The size of these domains is about 0.8 μm, which corresponds to the larger size peak in the SEM micrograph. The other consists of the darker portion only and can be attributed to the phase of the I-Zn added in excess for the encapsulation. The size of these domains is about 0.2 μm. These domains correspond to the smaller size peak in the SEM micrographs.

From these results, we can conclude as follows:

1. I-Zn is effective to compatibilize EBM and PET blends.
2. I-Zn encapsulates EBM in PET matrix. This result agreed well with the anticipation based on the above-mentioned concept.

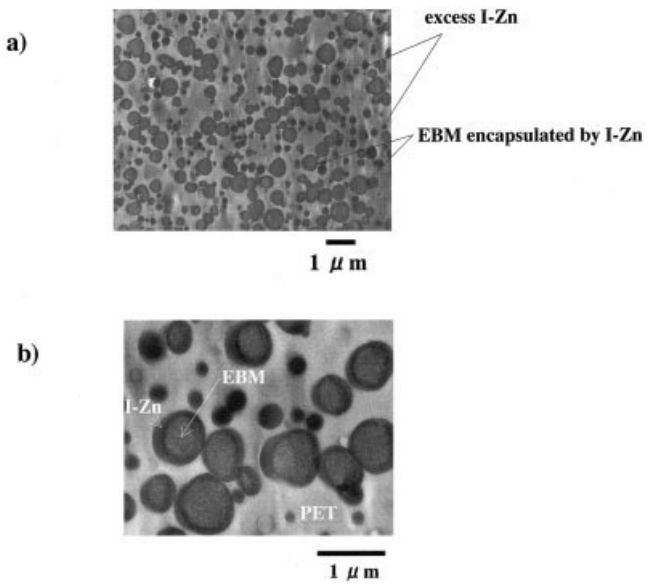

Figure 3 TEM micrographs of PET/EBM/I-Zn (80/10/10) blend. (a) Low and (b) high magnifications.

Morphologies in binary blends of the constituent polymers

To verify the driving force for the encapsulation experimentally, Figure 4 shows the dispersed domains in the binary blends consisting of the two constituent polymers. In binary polymer blend systems, morphology generation is usually discussed in terms of a balance between fluid drop burst and coagulation. By expanding the Taylor theory [26,27] for aqueous colloid to the viscoelastic field in polymer blends, the equivalent droplet size, d, is given by eq. (6):[28,29]

$$\eta_m G d / \gamma_{d/m} = F(\eta_d / \eta_m) \tag{6}$$

where $\gamma_{d/m}$ is the interfacial tension between the dispersed domains and matrix polymer; G is the shear rate; η_m and η_d are the viscosity of the matrix and the dispersed domains, respectively. Because all of these binary blends were melt mixed at the same conditions, G should be almost the same for these blends. In addition, when the effect of viscosity at a first approximation is ignored, the particle size, d, will be directly proportional to the interfacial tension:

$$d \sim \gamma_{d/m} \tag{7}$$

Equation (7) implies that $\gamma_{i/j}$ can be evaluated by the domain size in Figure 4. The large domains in the PET/EBM blend signify large $\gamma_{\mathrm{PET/EBM}}$, while the small domains in the blends of EBM/I-Zn and PET/I-Zn indicate small $\gamma_{\mathrm{EBM/I\text{-}Zn}}$ and $\gamma_{\mathrm{PET/I\text{-}Zn}}$, respectively. By substituting these evaluated γs into eq. (1), the left formula portion of eq. (1) becomes (large) – (small) – (small). These results suggest the spreading parameter, $\lambda_{\mathrm{I\text{-}Zn/EBM\ in\ PET}}$, actually becomes positive.

Results of droplet sandwich experiments

To clarify the driving force of encapsulation more pointedly, the droplet sandwich experiments were carried out, following the analysis proposed by Nakamura and Inoue[15] According to their analysis, when a liquid droplet of polymer ***1*** floats between the two liquid polymers of ***2*** and ***3***, the location and surface shape of ***1*** are determined by the balance of the interfacial tensions. As illustrated in Figure 5, there are three possible locations and shapes of a floating polymer depending upon the interfacial tension balance:[15,18] (a) thin phase of ***1*** spread between ***2*** and ***3***; (b) droplet of ***1*** buried in ***2***; and (c) droplet of ***1*** locating between ***2*** and ***3***.

In the case (a), the thin phase of ***1*** spreads between ***2*** and ***3***, because the contact of ***2*** and ***3*** is the most unstable among the possible connections between these polymers. This connection should be avoided in the actual ternary blend systems of ***1***, ***2***, and ***3***. Consequently, the capsule formation of Figure 1(b) will be developed, when the thin phase of ***1*** spreads between ***2*** and ***3*** as in Figure 5(a). Similarly, in the case (b) ***1***

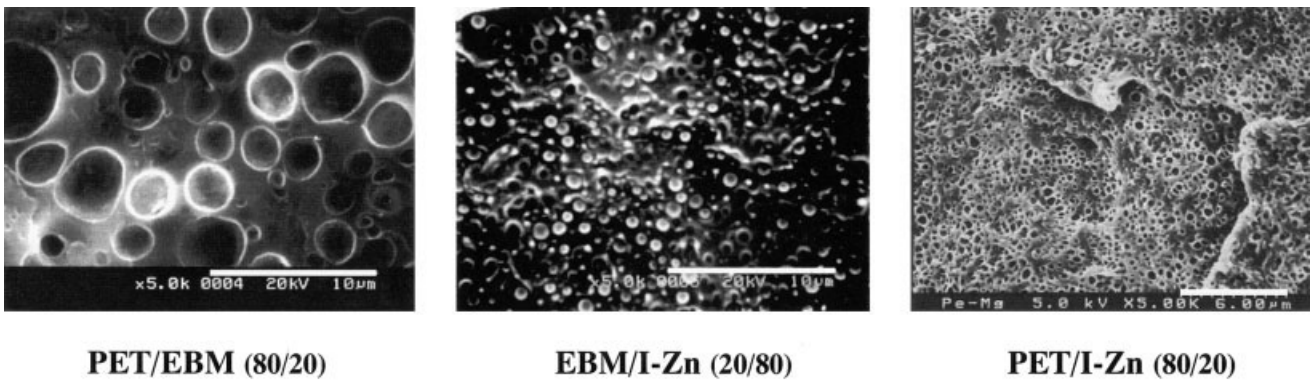

Figure 4 Phase morphology in the binary polymer blends of the constituent polymers.

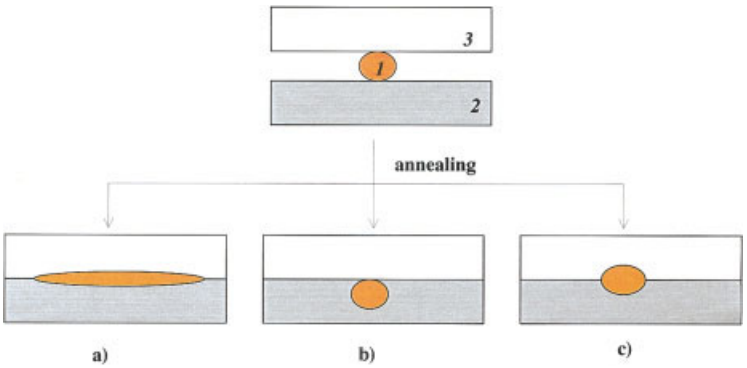

Figure 5 Possible location and shapes of the floating polymer. (a) Thin phase of polymer ***1*** spread between polymers ***2*** and ***3***; (b) droplet of ***1*** buried in ***2***; (c) droplet of ***1*** locating between ***2*** and ***3***.

buries in ***2***, because the contact between ***1*** and ***3*** is the most unstable. Thus, the capsule formation of ***1*** encapsulated by ***2*** will be developed when the matrix of the blend consists of ***3***. The situation is quite different in case (c). Because there is no large difference in stability among the possible contacts of these polymers, they can directly contact with each other. Thus, at case (c), the stack formation of Figure 1(a) will be predicted.

Figure 6 shows the cross sections of the droplet after the droplet-sandwich experiments. When small pieces of I-Zn were sandwiched between PET and EBM, a thin layer of the I-Zn widely spread between these polymers [Fig. 6(a)]. When the EBM droplets were sandwiched between PET and I-Zn, the EBM droplet is buried in the I-Zn [Fig. 6(b)]. These results indicate that the capsule formation where I-Zn encapsulates EBM in PET matrix should be developed. This perdition well agreed with the results of the TEM analysis.

From the results of the sandwich experiments and the spreading parameter evaluation, we can confirm experimentally the driving force for the encapsulation in the PET/EBM/I-Zn blend is wettability.

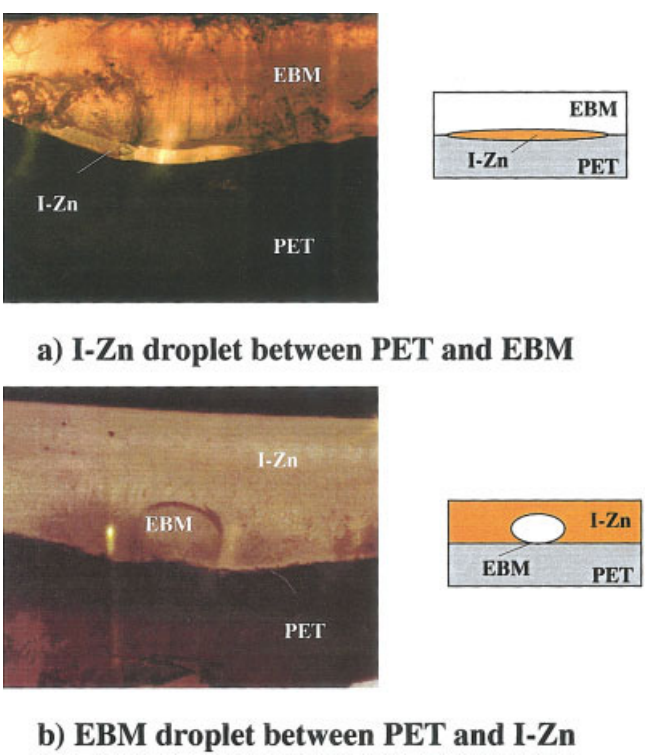

Figure 6 Cross sections of the droplet after annealing. (a) I-Zn droplet between PET and EBM; (b) EBM droplet between PET and I-Zn.

Role of polar units in I-Zn on encapsulation

To verify the design concept of chemistry for the encapsulating agent, the phase morphology in the PET/EBM/VLDPE blend was examined. Because VLDPE consists of nonpolar units only, the role of the polar units in I-Zn can be evaluated by comparison. Figure 7 shows the phase morphology in the binary blends of the constituent two polymers. The large domains are dispersed in both PET/EBM and PET/VLDPE blends. In addition, the size of the dispersed domains seems almost the same for these blends. Comparing the phase morphologies between the PET/VLDPE and the PET/I-Zn [Fig. 5(c)] blends, it was found that the polar units in I-Zn contribute to decrease $\gamma_{PET/I\text{-}Zn}$, while in the EBM/I-Zn blend fine domains are dispersed with a little smaller size than in the EBM/I-Zn blend [Fig. 5(b)]. This result indicates that the nonpolar units prevent the$\gamma_{EBM/I\text{-}Zn}$ from becoming too large, although the polar units in I-Zn increase $\gamma_{EBM/I\text{-}Zn}$ a little. By substituting the evaluated γs into eq. (1), the left formula portion should serve (large) − (small) − (large). Furthermore, the first and third term,$\gamma_{PET/LLDPE}$ and $\gamma_{PET/EBM}$, are evaluated almost the same. Consequently, the spreading parameter, $\lambda_{VLDPE/EBM\ in\ PET}$, should become minus and the stack formation is predicted. As actually shown in Figure 8, "stack formation," where EBM and VLDPE are stuck to each other, is developed in the PET/EBM/VLDPE blend.

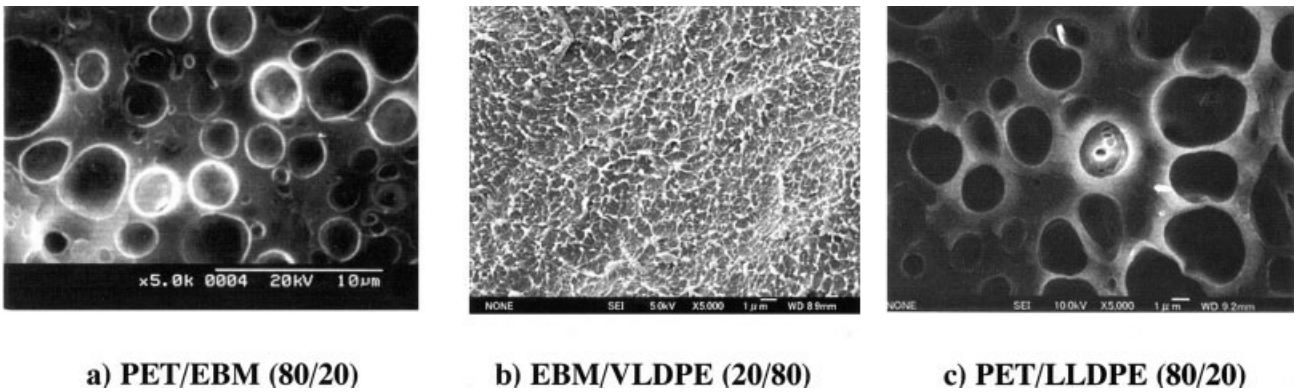

Figure 7 Phase morphology in the binary blends of the constituent polymers of PET, EBM, and LLDPE. (a) PET/EBM (80/20); (b) EBM/VLPDE (20/80); (c) PET/LLDPE (80/20).

From these results it the following can be concluded: I-Zn can encapsulate EBM in PET matrix by the contribution of the polar and nonpolar units to decrease $\gamma_{PET/I\text{-}Zn}$ and $\gamma_{EBM/I\text{-}Zn,}$ respectively. These results agreed well with the anticipation based on the repulsion idea in random copolymers. This agreement suggests that the repulsion idea is applicable for molecular design for an encapsulating agent.

Effects of neutralizing metal ions on compatibilization and encapsulation

To examine how metal ions affect the mechanisms of compatibilization and encapsulation, Figure 9 shows the SEM micrographs in the blends of PET, EBM, and ionomers, which are neutralized by different metal ions: I-Zn, I-Na, I-Mg, and unneutralized (EMAA).

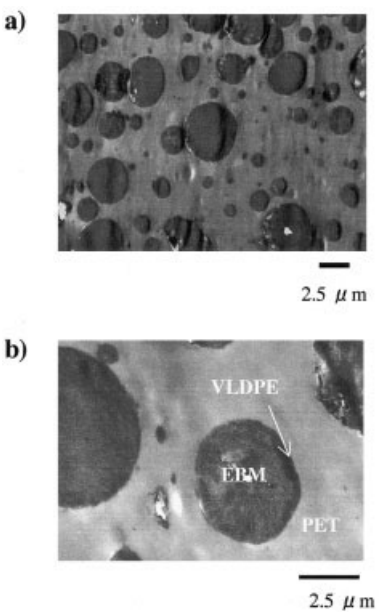

Figure 8 TEM micrographs of PET/EBM/VLDPE (80/10/10) blend. (a) Low and (b) high magnification.

When compatibilized by the ionomers [Figs. 9(a–c)], the domain size seems almost the same, although there is a small difference. The dispersed domains seem a little larger in the PET/EBM/I-Mg blend. However, the size is almost below 1 μm. These results signify that all of these ionomers can effectively compatibilize EBM and PET blends, regardless the kind of the neutralizing metal ions.

In the PET/EBM/EMAA blend, the size of the dispersed domains is much larger (about 2 μm), indicating that the unneutralized EMAA cannot effectively compatibilize EBM and PET blends. To examine the morphology formation, Figure 10 shows the TEM micrographs of the PET/EBM/EMAA blend. The "capsule formation" of EBM encapsulated by EMAA is developed, although the size of the dispersed phase is much larger than that in the PET/EBM/ionomer blends.

Combining the results of the previous section, we can conclude the following: Because the EMAA consists of both polar and nonpolar units, the EMAA can encapsulate the EBM in the PET matrix, independently of whether the EMAA is neutralized by metal ions. However, the neutralization of the EMAA has a great influence on the compatibilization. Only when neutralized can the EMAA effectively compatibilize EBM and PET blends, in addition, regardless of the kinds of neutralizing metal ions.

Compatibilization mechanism by ionomer

The compatibilization effectiveness of the ionomers could be traced to their strong adhesion to PET–a result of the interaction between PET and ionomers occurring at their interface when blended at high temperatures. The possible interactions are:

1. hydrogen bonding between –COOH in the ionomers and carbonyls in PET[30,31]

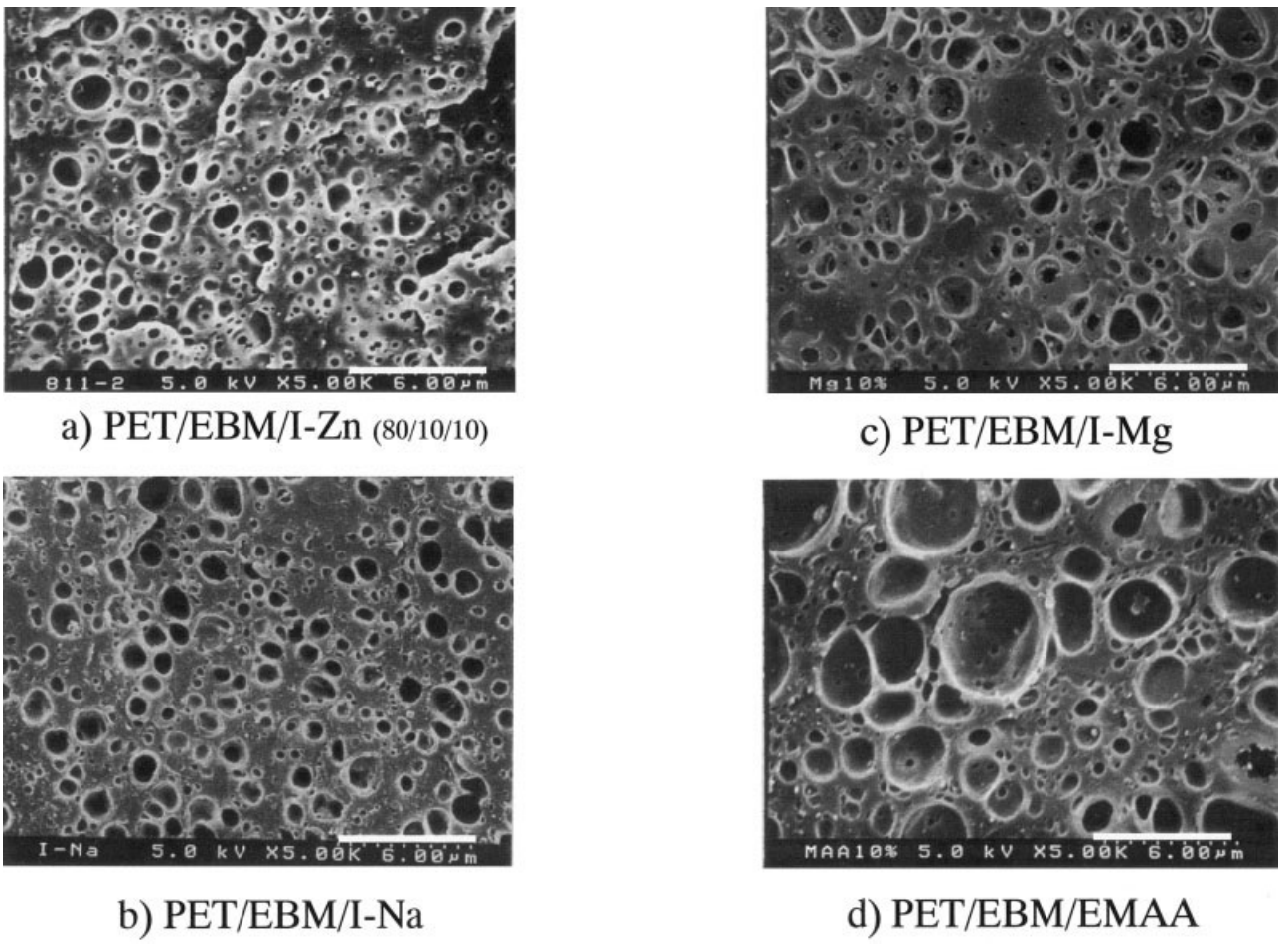

Figure 9 Phase morphology in PET and EBM blends compatibilized with ionomers, which are neutralized by different metal ions: (a) Zn^{2+}, (b) Na^{+}, (c) Mg^{2+}, and (d) unneutralized (EMAA).

2. transetherification between free carboxyls in the ionomers and ester units in PET[10,32,33]
3. transetherification between carboxyl salts in the ionomers and ester units in PET[10,32,33]
4. ionic interactions between the metal ions in the ionomers and –COOH in PET terminals
5. coordination of PET-carbonyls to the metal ions in the ionomers.

The former two interactions can occur between the free acid in the ionomers and PET, while the latter three are caused by the metal ions in the ionomers. Considering the results showing that the neutralized EMMA can more effectively compatibilize EBM and PET, the latter three seem more plausible. However, it is not clear which interaction actually occurs during the melt mixing process.

Once strong interaction between the ionomers and PET is obtained at the interface, the corona of the grafting PET will be developed[34] as shown in Figure 11. This corona will produce two driving forces to reduce the core shell domains consisting of EBM and

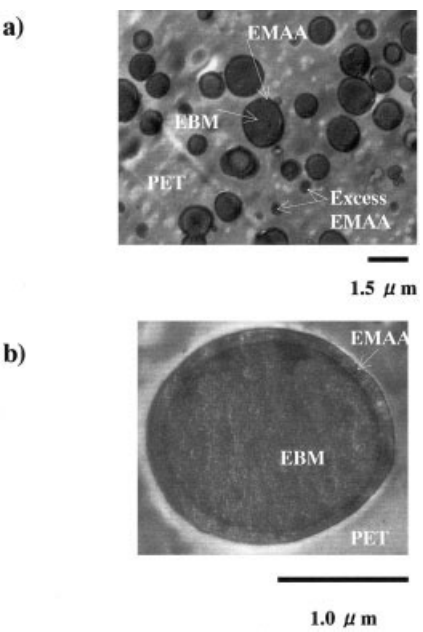

Figure 10 TEM micrographs of PET/EBM/EMAA (80/10/10) blend. (a) Low and (b) high magnification.

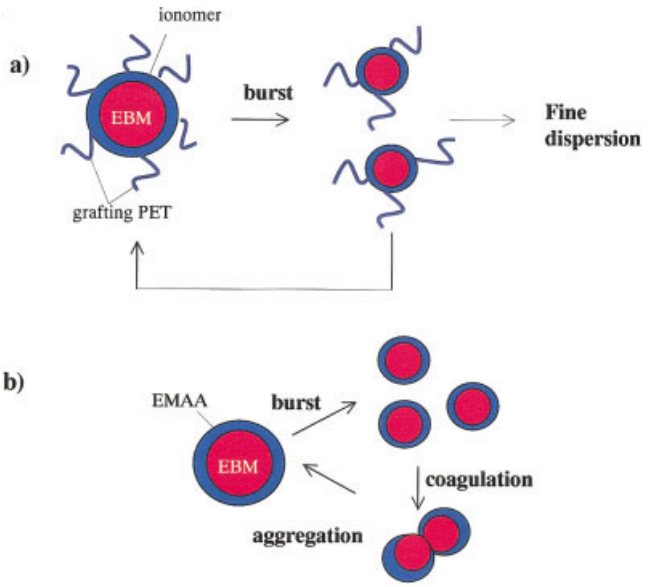

Figure 11 Concept figure of the compatibilization kinetics during the melt mixing process. (a) PET/EBM/ionomer (I-Zn, I-Na, I-Mg) and (b) PET/EBM/EMAA blends.

ionomers. One is stabilization of the interface between the ionomer and PET.[35] The other is coagulation depression of the core-shell droplets during the melt mixing process. Without any corona, the equivalent size of the core-shell droplets is determined by the kinetic balance between burst, coagulation, and aggregation during the melt mixing as shown in Figure 11(b).[26] Because the interactions between EMAA and PET are weak, the equivalent size of the core-shell droplets should be governed by these factors in the PET/EBM/EMAA blend. In the PET/EBM/ionomer blend, the coagulation of the core-shell droplets should be depressed by the grafting PET corona, and consequently the size of the dispersed domains will shift smaller.[36]

The ionomers are supposed to effectively compatibilize PET and EBM because of the grafting PET corona, which is developed via the strong interaction between PET and the ionomers.

CONCLUSION

The phase morphology and mechanism for compatibilization in ternary blends of PET/EBM/ionomer are examined. Applying the repulsion idea in a random copolymer, the ionomer was selected as an encapsulating agent to compatibilize PET and EBM blends. The main results and discussions are enumerated below:

1. I-Zn can encapsulate EBM in PET matrix and effectively compatibilize PET and EBM.
2. The results of the phase morphology analysis in the binary blends of the constituent polymers suggest the spreading parameter $\lambda_{\text{I-Zn/EBM in PET}}$ actually becomes positive. In addition, the droplet sandwich experiment results predict that the "capsule formation" of EBM encapsulated by I-Zn is developed in the ternary blend of PET/EBM/I-Zn. From these results, the actual driving force for the encapsulation is experimentally confirmed wettability.
3. From the comparison with the phase morphology in the PET/EBM/VLDPE blend, the polar and nonpolar units in I-Zn were found to contribute to decreased $\gamma_{\text{PET/I-Zn}}$ and $\gamma_{\text{EBM/I-Zn}}$, respectively, and make the encapsulation possible. These results agreed well with the anticipation based on the repulsion idea in random copolymers. This agreement suggests that the repulsion idea is adjustable to the molecular design for an encapsulating agent.
4. The metal ions in the ionomer, on the other hand, have little influence on the encapsulation. EMAA can encapsulate EBM even when unneutralized. However, the compatibilization efficiency is not determined by the encapsulation only. The metal ions have a great influence on the compatibilization efficiency. Only when neutralized can EMAA effectively compatibilize EBM and PET, in addition, regardless of the kind of metal ions.
5. The compatibilization effectiveness of conclusion 4 is supposedly due to the strong interaction between PET and the metal ions.

The author is grateful to Mrs. K Niki, Y. Noumi, and Y. Kikuchi of the Technical Support Center of Nippon Steel Corp. Japan for technical assistance in the melt mixing operation and taking the SEM micrographs. Also, the author thanks Mr. K. Nakakaze of Mishima Kosan Co. Japan for kind help in preparing the specimens for the SEM micrographs.

References

1. Paul, D. R. Polymer Blends; Academic Press: San Diego, CA, 1978; vols. 1 and 2.
2. Olabisi, O.; Robeson, L. M.; Shaw, M. T. Polymer–Polymer Miscibility; Academic Press: San Diego, CA, 1979.
3. Nishi, T.; Akiyam, S.; Inoue, T. Polymer Blends; CMC Press: Tokyo, Japan, 1981.
4. Kotaka, T., Ed. Polymer Alloy; Tokyo: Kagakudojin, 1993; 2nd ed.
5. Utracki, L. A. Polymer Alloys and Blends; C. Hanser: Munich, 1990.
6. Tanaka, A.; Hanafusa, T.; Kojyo, H.; Inui, T. Tetsu-to-Hagane 1986, 72, 1189.
7. Maida, T. Zairyo-to-Kankyo 2000, 49, 669.
8. Matsubayashi, H. Zairyo-to-Kankyou 2002, 51, 299.
9. Traugott, T. D.; Barlow, J. W.; Paul, D. R. J Appl Polym Sci 1983, 28, 2947.

10. Kalfoglou, N. N.; Skafidas, D. S.; Kallitsis, J. K.; Lambert, J. C.; Stappen, L. V. Polymer 1995, 36, 4453.
11. Torres, N.; Robin, J. J.; Boutivin, B. J Appl Polym Sci Vol 2001, 81, 2377.
12. Luinchi, J. M.; Torres, N.; Robin, J. J.; Boutevin, B. J Appl Polym Sci 2001, 79, 874.
13. Pluta, M.; Bartczak, Z.; Pawlak, A.; Galeski, A.; Pracella, M. J Appl Polym Sci 2001, 82, 1423.
14. Hobbs, S. Y.; Dekkers, M. E. J.; Watkins, V. H. Polymer 1988, 29, 1598.
15. Nakamura, G.; Inoue, T. Koubunshi Ronbunsyu 1990, 47, 409.
16. Horiuchi, S.; Mahcariayakul, N.; Yase, K.; Kitano, T.; Choi, H. K.; Yee, Y. M. Polymer 1996, 37, 3065.
17. Horiuchi, S.; Mahcariayakul, N.; Yase, K.; Kitano, T.; Choi, H. K.; Yee, Y. M. Polymer 1997, 38, 59.
18. Horiguchi, S.; Mahcariayakul, N.; Yase, K.; Kitano, T. Macromolecules 1997, 30, 3664.
19. Helfand E.; Tagami, Y. J Polym Sci, Part B: Polym Phys 1971, 9, 741.
20. Helfand, E.; Tagami, Y. J Chem Phys 1969, 56, 3592.
21. ten Brinke, G.; Karasz, F. E.; MacKnight, W. J. Macromolecules 1983, 16, 1827.
22. Bauer, B. J. Polym Eng Sci 1985, 25, 1081.
23. Kammer, H. W. Acta Polym 1986, 37, 1.
24. Suess, M.; Kressler, J.; Kammer, H. W. Polymer 1987, 28, 957.
25. Ohishi, H.; Kishimoto, S.; Ikehara, T.; Nishi, T. J Polym Sci, Part B: Polym Phys 2000, 38, 127.
26. Taylor, G. I. Proc R Soc Lond A 1932, 138, 41.
27. Taylor, G. I. Proc R Soc Lond A 1934, 139, 501.
28. Wu, S. Polym Eng Sci 1987, 27, 335.
29. Serpe, G.; Jarrin, J.; Dawans, F. Polym Eng Sci 1990, 30, 553.
30. Guerrero, C.; Lozano, T.; Gonzalez, V.; Arroyo, E. J Appl Polym Sci 2001, 82, 1382.
31. Retolaza, A.; Eguiazabal, J. I.; Nazabal, J. Polym Eng Sci 2002, 42, 2072.
32. Yu, Y.; Bu, H. Macromol Chem Phys 2001, 202, 421.
33. Sanches, N. B.; Pacheco, E. B.; Dias, M. L. ANTEC 2002, 60, 4014.
34. Kotaka, T., Ed. Polymer Alloy; Tokyo: Kagakudojin, 1993; 2nd ed, p. 358.
35. Patterson, H. T.; Hut, K. H.; Grindstaff, T. H. J Polym Sci, Part C 1971, 34, 31.
36. Sundaraj, U.; Macosko, C. W. Macramolecules 1995, 28, 2647.